

On the relation between magnetic perturbations induced toroidal asymmetries and the pump-out effect in ASDEX Upgrade

Nils Leuthold¹, W. Suttrop¹, M. Willensdorfer¹, M. Cavedon¹, M. Dunne¹, L. Gil², T. Happel¹, A. Kirk³, P. Manz¹, J. Vicente², the ASDEX Upgrade⁴ and MST1⁵ teams

¹*Max Planck Institute for Plasma Physics, Boltzmannstrasse 2, 85748 Garching, Germany*

²*Instituto de Plasmas e Fusao Nuclear, Instituto Superior Tecnico, Universidade de Lisboa, Portugal*

³*CCFE, Culham Science Centre, Abingdon, Oxon, OX14 3DB, U.K.* ⁴*See A. Kallenbach et al, Nucl. Fusion 57 (2017) 102015* ⁵*See H. Meyer et al, Nucl. Fusion 57 (2017) 102014*

Introduction When a critical heating power is reached in a tokamak, the plasma transitions from the low- to the high-confinement mode. In this regime, turbulent transport is reduced at the edge forming a transport barrier, which produces a region of steep gradients at the plasma edge and a significantly increased density and temperature in the core plasma. While the increased confinement of this regime has been taken into account for the design of the next generation fusion experiment ITER to accomplish its objectives, the steep gradients in the transport barrier lead to Edge-Localized-Modes (ELMs), which expel particles and energy in a pulsed manner. In order to reduce the erosion of the first wall material in ITER, those ELMs have to be mitigated or suppressed. One tool for ELM control being installed in ITER are Magnetic Perturbation (MP) coils, which break the 2D symmetry of the confining magnetic field (fig. 1 shows the ASDEX Upgrade MP coil set). Mitigation and suppression of ELMs via MPs was successfully demonstrated already in several devices [1,2,3]. However in scenarios with ITER-like collisionality, MPs also trigger the so called 'pump-out' effect in ASDEX Upgrade: an increase of the outward particle and heat transport, which causes the density to drop significantly (up to 50%) while the temperature stays roughly constant. The resulting pressure reduction leads to a confinement loss, which hopefully can be minimized or even avoided in ITER. In this paper, we study the toroidal asymmetry induced by MPs and a possible mechanism for increased outward transport across the edge barrier.

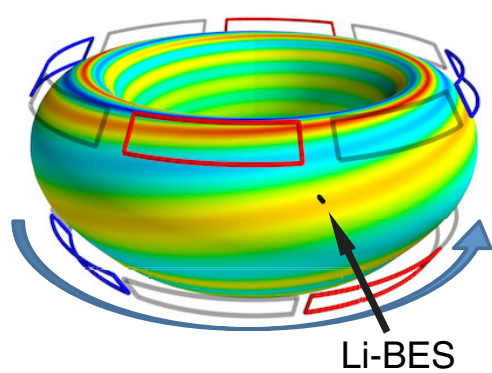


Figure 1: MP coil setup on ASDEX Upgrade. The plasma surface displacement with respect to the axisymmetric equilibrium calculated by VMEC points outward in the red, inward in the blue and is zero in the green area. Included is the position of the Li-Beam Emission Spectroscopy. [4]

Experimental setup In order to avoid the perturbations by ELMs, we choose the recently developed ELM suppression scenario for our experiment [2]: toroidal magnetic field $B_t = -1.8$ T, plasma current $I_p = 0.9$ MA, edge safety factor $q_{95} = 3.65$, upper triangularity $\delta_u = 0.479$. In discharge #34548 (see fig. 2), the MP coils are switched on at $t = 1.5$ s just after the ramp-up and once the density dropped below $3.3 \cdot 10^{19} \text{ m}^{-3}$ the transition into ELM suppression takes place at $t = 2.7$ s. We consider a case with rigid rotation ($f = 0.5$ Hz) of the $n = 2$ magnetic perturbation from $t = 3.0$ to 7.0 s, which allows for two complete rotation periods. This discharge was designed to be as stationary as possible in this phase, but yet some variations can be identified. First, at $t = 4.4$ s the sawtooth crashes vanish and the core temperature drops. Second, starting at the same time, the electron density is slowly increasing in the whole plasma. When the MP field is rotating, a diagnostic fixed in space will measure at positions of varying surface corrugation (fig. 1). Tracking a certain density (fig. 3(a)) and ion temperature (fig. 3(b)) close to the separatrix reveals the corrugation of the plasma. In addition, the simulated separatrix position by VMEC [5] is shown in order to allow a comparison with other diagnostics, which don't reveal the surface corrugation themselves. To make the measured and simulated separatrix position fit, first, a shift in radial direction is necessary, which is quite natural since the exact value at the separatrix to track in the diagnostic is not known and also the VMEC equilibrium itself might need to be shifted slightly as a whole. On the other hand, a phase shift is still present even after correcting for radial plasma movements induced by the plasma control system in response to $n = 2$ pick-up in its poloidal field sensors [6]. The reason for it is not known yet. The four different phases marked in fig. 3 are labelled corrugation minimum (blue), increasing flank zero crossing (red), corrugation maximum (green) and decreasing flank zero crossing (black), respectively. In the further analysis those phases are referred to as positions in the corrugation and measurements in those phases are compared.

Toroidally asymmetric gradients The corrugation of the magnetic field leads not only to a shift of the kinetic profiles but also to a variation of their gradients. The reason

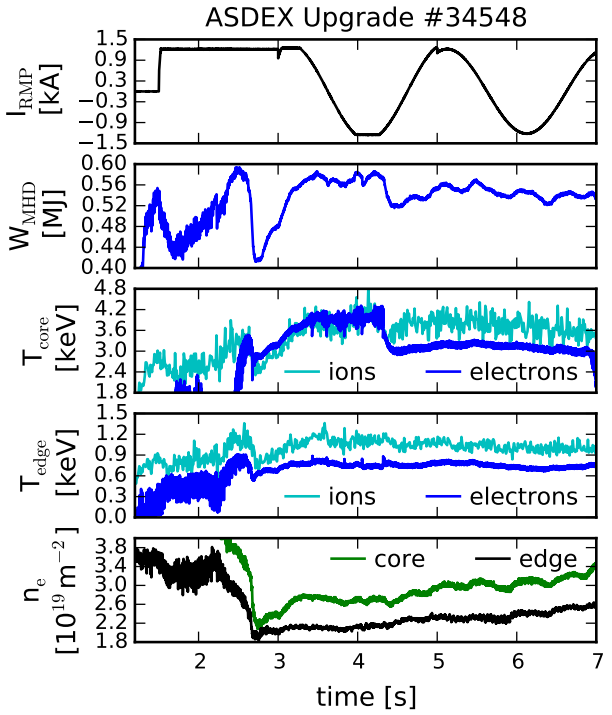


Figure 2: Timetraces of #34548: current in one of the RMP coils I_{RMP} , plasma stored energy W_{MHD} , temperature in the core T_{core} and edge T_{edge} region near the pedestal top for both species, line integrated electron density in the core n_{core} and edge n_{edge} region.

in the whole plasma. When the MP field is rotating, a diagnostic fixed in space will measure at positions of varying surface corrugation (fig. 1). Tracking a certain density (fig. 3(a)) and ion temperature (fig. 3(b)) close to the separatrix reveals the corrugation of the plasma. In addition, the simulated separatrix position by VMEC [5] is shown in order to allow a comparison with other diagnostics, which don't reveal the surface corrugation themselves. To make the measured and simulated separatrix position fit, first, a shift in radial direction is necessary, which is quite natural since the exact value at the separatrix to track in the diagnostic is not known and also the VMEC equilibrium itself might need to be shifted slightly as a whole. On the other hand, a phase shift is still present even after correcting for radial plasma movements induced by the plasma control system in response to $n = 2$ pick-up in its poloidal field sensors [6]. The reason for it is not known yet. The four different phases marked in fig. 3 are labelled corrugation minimum (blue), increasing flank zero crossing (red), corrugation maximum (green) and decreasing flank zero crossing (black), respectively. In the further analysis those phases are referred to as positions in the corrugation and measurements in those phases are compared.

is the compression of the flux surfaces in the corrugation minimum and the expansion in the maximum. The normalized inverse gradient length a/L_x with minor radius a and $L_x = \frac{x}{\nabla x}$ is shown for both, the electron density and ion temperature (fig. 4) as a function of distance to the separatrix. Compared to the profiles of a/L_{n_e} in the flanks, an increase of about 50 % in the corrugation minimum and a decrease of about 35 % in the corrugation maximum can be observed for the electron density. A similar behavior is seen in the ion temperature, although with larger gradients and error bars of the measurement.

Toroidally asymmetric density fluctuations In ASDEX Upgrade the Frequency Modulated Continuous Wavelength Reflectometer [7] can be run at fixed frequencies in O-mode in order to measure density fluctuations at a certain density. The K-band was set to 18 GHz and the Ka-band to 37 GHz, which correspond to 0.4 and $1.7 \cdot 10^{19} \text{ m}^{-3}$, respectively (see. fig. 6).

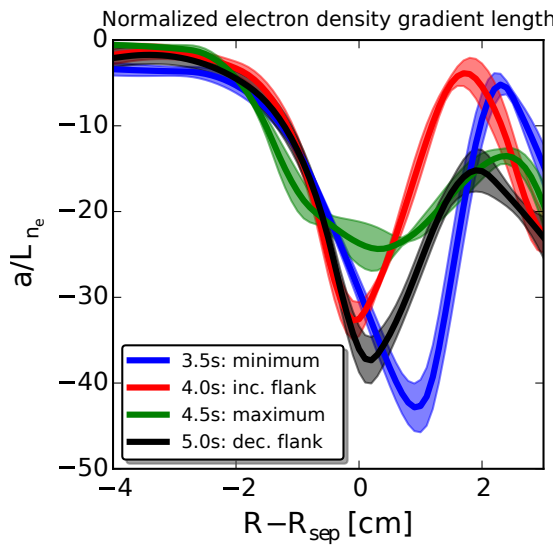


Figure 4: Normalized gradients length of the electron density (left) and ion temperature (right) for different positions in the corrugation (referring to the red line in fig. 3).

In the spectrograms of both bands (fig. 5) one small window of reduced fluctuation level is present per rotation period. In the Ka-band they appear always on the decreasing flank and with the lowest turbulence level achieved half way towards the corrugation minimum. At this position, a weak reduction of turbulence is also seen in the K-band,

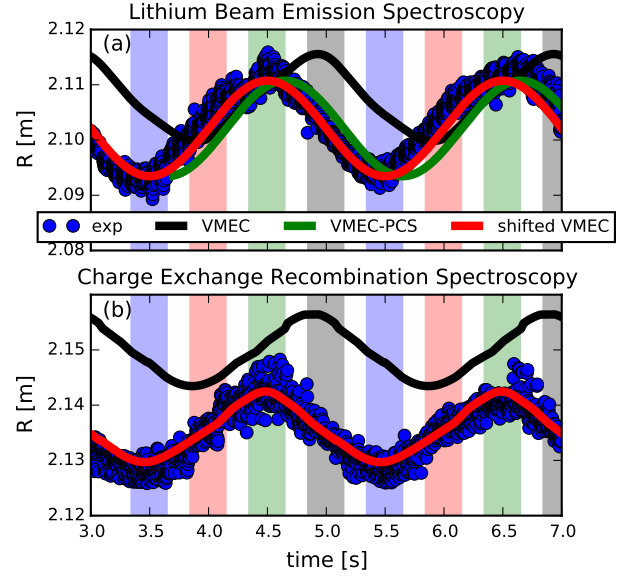


Figure 3: Time traces of the corrugation in the line-of-sights of the Lithium Beam Emission (a) and Charge Exchange Recombination (b) Spectroscopy.

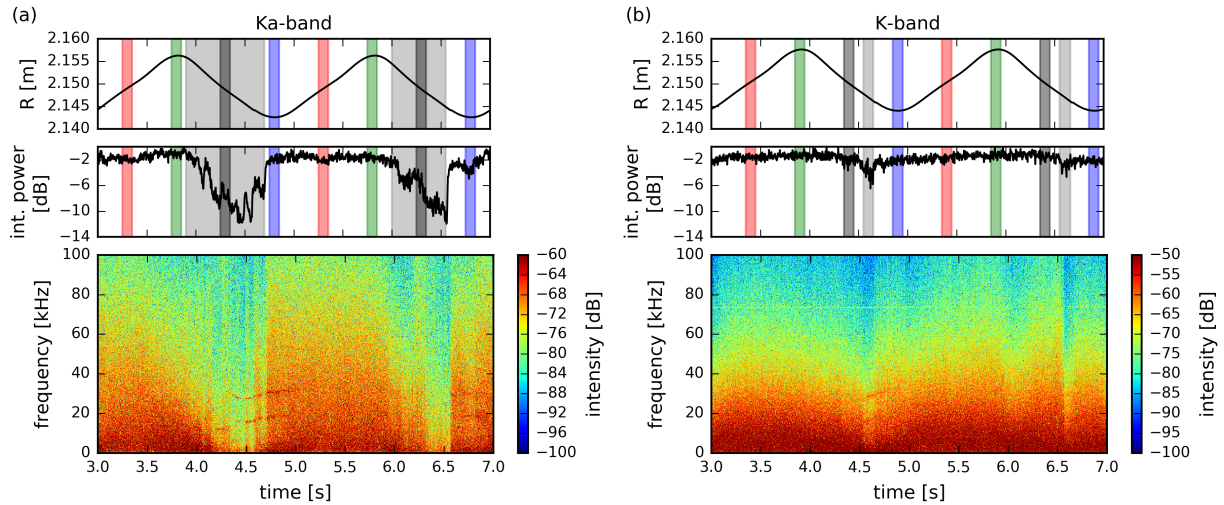


Figure 5: The simulated and shifted separatrix position (top), integrated power (middle) and spectrogram (bottom) of the Ka-band (a) and K-band (b) reflectometry. The color code refers to fig 3 and fig. 4, the light grey shaded area is where the integrated power drops.

although in a narrower toroidal phase range. On the other hand, the high turbulence on the increasing flank could contribute to the pump-out effect. It is remarkable that the lowest turbulence level does not occur in the corrugation maximum, where the gradients are lowest, although curvature may play a role. Furthermore, turbulence stabilization due to v_{ExB} shear can also not be the only reason for the localization of the turbulence, since the v_{ExB} shear is maximal in the corrugation minimum. The reason for that is not only the steeper gradient, but also a more negative E well. Assuming that the plasma potential, averaged over long time scales of the perturbation field rotation, stays constant on flux surfaces - which is a fair assumption due to the high temperature - the absolute E_r minimum has to increase according to $E_r = -\nabla\phi$.

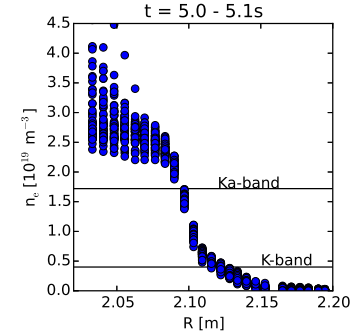


Figure 6: Illustration of the reflectometry reflection positions of the K- and Ka-band. While the K-band measures in the scrape-off-layer, the Ka-band observes the steepest gradients region, where the H-mode transport barrier is located.

- [1] T. Evans *et al* Plasma Fusion Res. **7** (2012) 2402046
- [2] W. Suttrop *et al*, arXiv:1804.00933 (accepted by Nucl. Fusion)
- [3] Y.M. Jeon *et al*, Phys. Rev. Lett. **109** (2012) 035004
- [4] M. Willensdorfer *et al*, Phys. Rev. Lett. **119** (2017) 085002
- [5] S.P. Hirshman *et al*, Phys. Fluids **26** (1983) 3553
- [6] M. Willensdorfer *et al*, Nucl. Fusion **57** (2017) 116047

- [7] A. Silva *et al*, Rev. Sci. Instrum. **70** (1999) 1072

This work has been carried out within the framework of

the EUROfusion Consortium and has received funding from the Euratom research and training programme 20142018 under Grant Agreement No. 633053. The views and opinions expressed herein do not necessarily reflect those of the European Commission.